Analytical, Computational, and Experimental Study of Discharge Plasma Capillaries for Laser Plasma Wakefield Acceleration

Mostafa Behtouei
Alicia Vázquez, Carlos Salgado López, Giancarlo Gatti

CLPU, Spain

November 7, 2025

Overview

- **Analytical:**
  - **Goal:** Characterize multi-mode laser–plasma interactions in capillary discharges.
  - **Method:** Operator-based framework.
  - **Key idea:** Separate "perturbative effects" (small imperfections) from "nonlinear dynamics" (laser–plasma feedback), then describe both using "operators".
- **Numerical:**
  - CFD simulation of gas flow and electron density profiles inside the capillary.
  - Optimization of capillary geometry for stable laser guiding.
- **Experimental:**
  - Design and realization of the setup for electron density diagnostics using Stark broadening.
  - Measurement and analysis of electron density in capillary discharges via Stark effect.

Perturbative vs Nonlinear Parts

Perturbative (Small imperfections)

- Linear mode coupling due to wall roughness, density fluctuations or turbulence or shot-to-shot variations in plasma formation
- Energy exchange between laser modes
- Treated using first-order corrections

Nonlinear (Laser-plasma feedback)

- Ponderomotive force drives plasma oscillations
- Plasma modifies laser via self-consistent nonlinear coupling
- Required for strong laser pulses and large-amplitude wakes

Bridge: From Dynamics to Operators

- Both perturbative and nonlinear dynamics can be expressed in a compact operator formalism.
- Define mode states:

$$|\Psi\rangle = \sum_n A_n |\psi_n\rangle, \quad |\delta n\rangle = \sum_m \delta n_m |\phi_m\rangle$$

- The "four key operators" appear naturally in the evolution equations:

$$i\partial_z |\Psi\rangle = \underbrace{\hat{K}}_{\text{perturbative}} |\Psi\rangle - \frac{\omega_0^2}{2k_0 c^2} \underbrace{\hat{N}[|\Psi\rangle]}_{\text{nonlinear feedback}} |\Psi\rangle$$

$$|\ddot{\delta n}\rangle + \underbrace{\hat{\Omega}_p^2}_{\text{plasma oscillations}} |\delta n\rangle = - \underbrace{\hat{\alpha}}_{\text{ponderomotive drive}} |\Psi|^2$$

- Linear perturbations ($\hat{K}$), nonlinear feedback ($\hat{N}$, $\hat{\alpha}$), and natural plasma oscillations ($\hat{\Omega}_p^2$) are all clearly included.

Laser and Plasma Modes with Operator Effects

$$|\Psi(z,t)\rangle = \sum_n A_n(z,t)\,|\psi_n\rangle\,, \quad |\delta n\rangle = \sum_m \delta n_m\,|\phi_m\rangle$$

- A_n: slowly-varying laser envelope amplitude (affected by $\hat{K}$ and $\hat{N}$).
- ψ_n: transverse laser modes shaped by the capillary.
- δn_m: plasma mode amplitudes (driven by $\hat{\alpha}$, oscillate with $\hat{\Omega}_p^2$).
- ϕ_m: radial plasma mode functions.
- Operator summary:
  - $\hat{K}$: linear perturbative mode coupling due to imperfections (Linear operator)
  - $\hat{N}$: nonlinear plasma feedback depending on laser intensity (Nonlinear operator)
  - $\hat{\Omega}_p^2$: natural plasma oscillations which contains information about plasma oscillation eigenfrequencies (Hermitian operator)
  - $\hat{\alpha}$: ponderomotive driving of plasma modes (Source operator)

Linear Imperfection Operator $\hat{K}$

To construct $\hat{K}$, we expand the system in a complete set of transverse modes $\{\psi_n(\mathbf{r})\}$ and project the dielectric perturbation $\Delta\epsilon(\mathbf{r}) = \epsilon(\mathbf{r}) - \epsilon_0$ onto this basis:

$$\kappa_{nm} = -\frac{\omega_0^2}{2} \int \psi_n^*(\mathbf{r})\, \Delta\epsilon(\mathbf{r})\, \psi_m(\mathbf{r})\, d^2r, \quad \hat{K} = \sum_{n,m} \kappa_{nm} \left|\psi_n\right\rangle \left\langle\psi_m\right|.$$

If $\Delta\epsilon(\mathbf{r})$ is real, $\hat{K}$ is Hermitian, ensuring energy-conserving linear coupling and real eigenvalues, so the propagation remains stable in the linear regime.

- Diagonal: phase shifts of laser modes.
- Off-diagonal: energy transfer due to imperfections.
- Treated perturbatively, small effect on evolution.
- Projecting this perturbation onto the modal basis yields the matrix elements which quantify the coupling of mode m into mode n.

Nonlinear Plasma Operator $\hat{N}$

The operator $\hat{N}$ describes the plasma response to laser intensity. Projecting the ponderomotive density perturbation $\tilde{n}(\mathbf{r}, z, t)$ onto the transverse modes gives

$$\mathcal{N}_{nm}(z,t) = \int \psi_n^*(\mathbf{r})\, \tilde{n}(\mathbf{r}, z, t)\, \psi_m(\mathbf{r})\, d^2 r, \quad \hat{N} = \sum_{n,m} \mathcal{N}_{nm} \left|\psi_n\right\rangle \left\langle\psi_m\right|.$$

Acting on $|\Psi\rangle = \sum_n A_n |\psi_n\rangle$:

$$(\hat{N}\Psi)_n = \sum_m \mathcal{N}_{nm} A_m,$$

with diagonal elements $\rightarrow$ self-modulation, off-diagonal $\rightarrow$ cross-mode energy transfer. Numerical evaluation produces a Hermitian matrix for coupled-mode propagation.

- Represents ponderomotive feedback: plasma modifies laser.
- Nonlinear: depends on laser amplitude A_n.
- Fully self-consistent for strong pulses, , meaning the laser and plasma evolve together in a fully coupled way.

Plasma Oscillation Operator $\hat{\Omega}_p^2$

The operator $\hat{\Omega}_p^2$ represents intrinsic electron oscillations in the plasma guiding structure.

Mode expansion:

$$\delta n(\mathbf{r}, z, t) = \sum_m \delta n_m(z, t)\phi_m(\mathbf{r}), \quad \nabla_\perp^2 \phi_m + \frac{\omega_{p,m}^2}{v_s^2}\phi_m = 0$$

Dynamics:

- Unperturbed: $\ddot{\delta n}_m + \omega_{p,m}^2 \delta n_m = 0$
- Laser-driven (ponderomotive force):

$$\ddot{\delta n}_m + \omega_{p,m}^2 \delta n_m = \int \phi_m^* \mathbf{F}_p \, d^2 r, \quad \mathbf{F}_p = -\nabla U_p, \quad U_p = \frac{e^2}{4 m_e \omega_0^2} |E|^2$$

Operator form:

$$\hat{\Omega}_p^2 \, |\delta n\rangle = \sum_m \omega_{p,m}^2 \delta n_m \, |\phi_m\rangle$$

Diagonal, Hermitian, and preserves mode orthonormality — convenient for coupled-mode propagation.

Ponderomotive Source Operator $\hat{\alpha}$

The ponderomotive source operator $\hat{\alpha}$ maps the laser-induced driving onto the plasma modes:

$$\hat{\alpha} = \sum_m \alpha_m \left|\phi_m\right\rangle \left\langle\phi_m\right|, \quad \left(\hat{\alpha}\left|\Psi\right\rangle^2\right)_m = \alpha_m \int \phi_m^* |\Psi|^2 \, d^2r$$

Complete plasma evolution equation:

$$\left|\ddot{\delta n}\right\rangle + \hat{\Omega}_p^2 \left|\delta n\right\rangle = -\hat{\alpha}\left|\Psi\right\rangle^2$$

This form clearly separates intrinsic oscillations ($\hat{\Omega}_p^2$) from the laser-driven source, ($\hat{\alpha}$), allowing a compact and numerically convenient description of plasma dynamics.

It describes how the laser drives the plasma modes, essentially mapping the laser intensity onto the plasma eigenmodes.

Coupled Evolution Equations

$$i\partial_z |\Psi\rangle = \hat{K} |\Psi\rangle - \frac{\omega_0^2}{2k_0 c^2} \hat{N}[\Psi] |\Psi\rangle$$

$$|\ddot{\delta n}\rangle + \hat{\Omega}_p^2 |\delta n\rangle = -\hat{\alpha}|\Psi|^2$$

- Feedback loop:
  - Laser $\rightarrow$ plasma: $\hat{\alpha}$
  - Plasma $\rightarrow$ laser: $\hat{N}$
  - Natural evolution: $\hat{K}$, $\hat{\Omega}_p^2$
- Operators: $\hat{K}$: linear imperfections, $\hat{N}$: nonlinear plasma feedback, $\hat{\Omega}_p^2$: plasma oscillations, $\hat{\alpha}$: ponderomotive drive
- Clearly separates perturbative and nonlinear contributions.

Neutral gas density study using CFD simulations in ANSYS Fluent to optimize the gas flow and density profile inside the capillary

How the shape affects gas flow and density distribution.

Neutral density study

1º Geometry models: *DesignModeller*

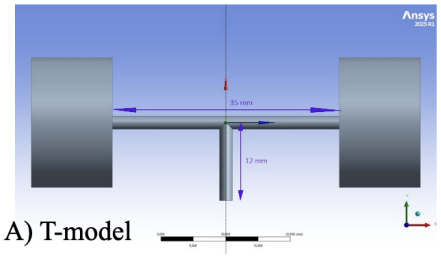

A) T-model

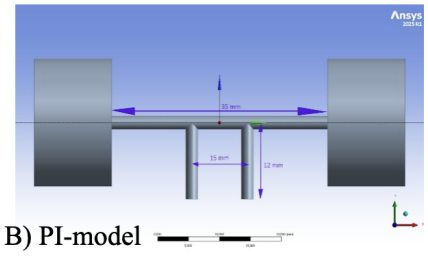

B) PI-model

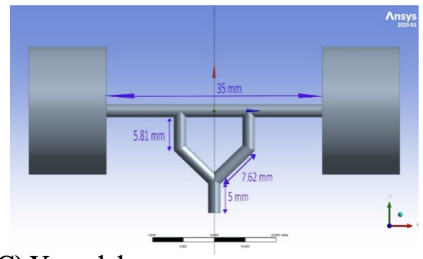

C) Y-model

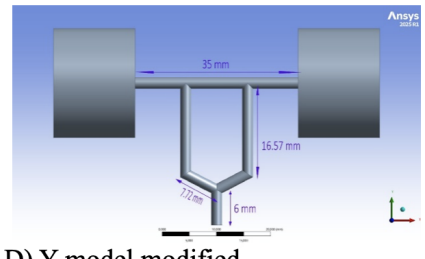

D) Y-model modified

2º Mesh definition: *Fluent*

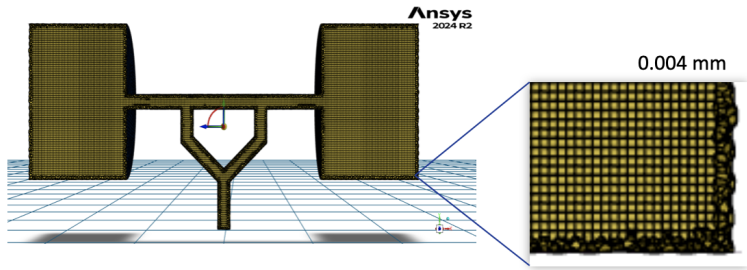

3º Problem boundary conditions: *Fluent*

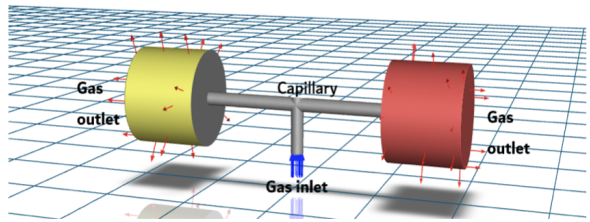

Boundary conditions were defined with gas inlets and outlets at both ends, allowing the simulation of steady-state neutral gas flow through the capillary.

The Y-model shows the most uniform and controllable density distribution, making it the best candidate for laser–plasma experiments.

The neutral density can be tuned by varying gas pressure

Neutral density study

Goals:

- Estimate gas density using different gas pressures and geometries.
- Model the density profile by varying geometry and pressure inlet.

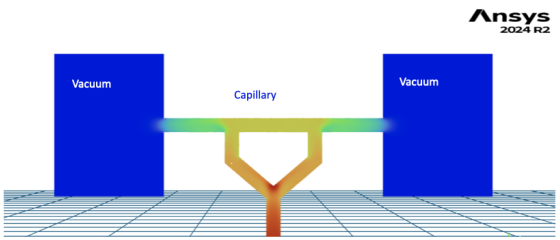

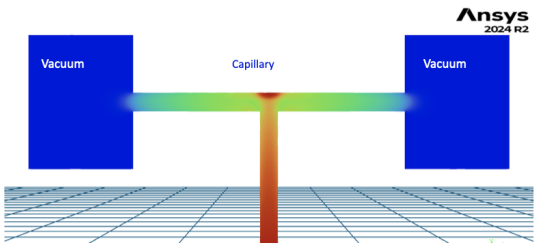

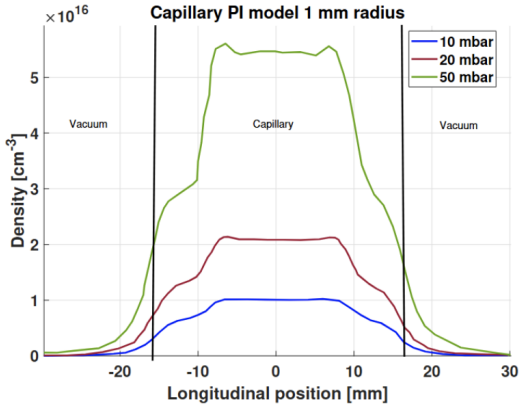

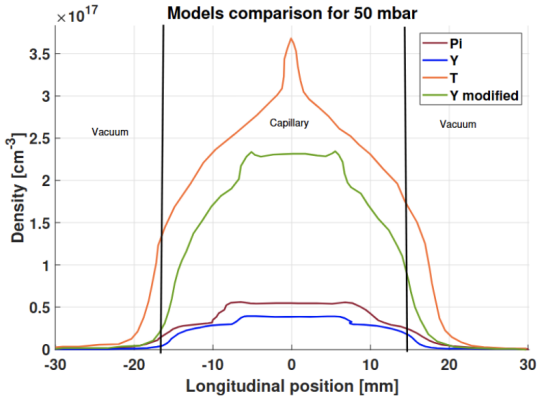

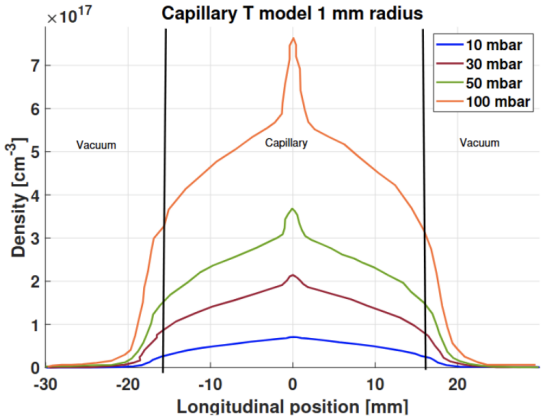

Conclusions:

- Neutral density tuneable with gas pressure.
- Y model results in the most homogeneous profile.

4. Experimental setup for the electronic density diagnosis using Stark broadening

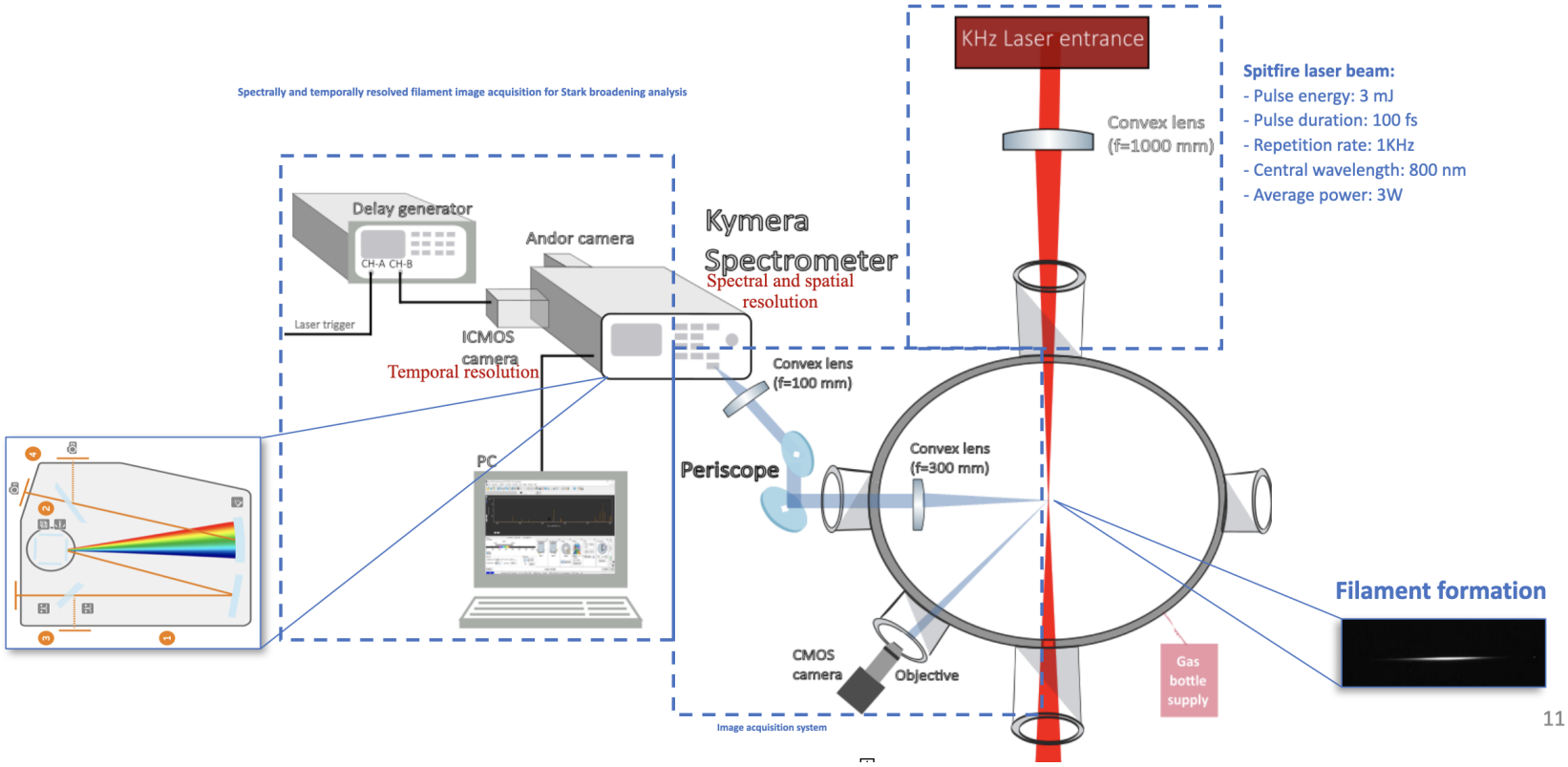

Experimental Layout

- **Laser system:** Ti:Sapphire laser (3mJ, 100fs, 800nm, 1kHz) generates plasma filament inside the capillary.
- **Optical path:** Beam focused by lenses and periscope into gas-filled chamber for controlled plasma formation.
- **Diagnostic system:** Emission collected by objective → Kymera spectrometer → ICMOS camera for Stark broadening analysis.

4. Experimental setup for the electronic density diagnosis using Stark broadening

Plasma source: **filament** induced by laser

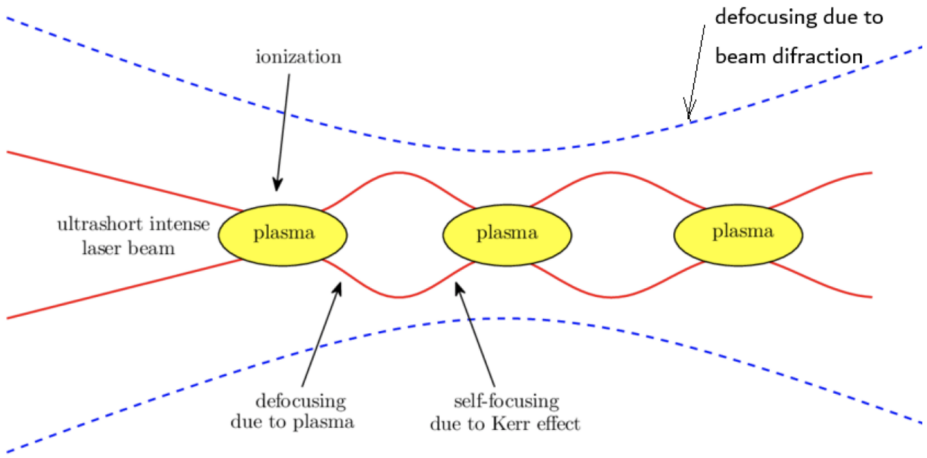

Competing effects:

- Kerr effect:

$$\eta = \eta_0 + \eta_2 I$$

Gas refractive index

- Ionization induced defocusing:

$$\eta_p = \sqrt{1 - \frac{n_e}{n_c}}$$

Plasma refractive index

Laser-Induced Filament Formation

- **Concept:** Plasma filament forms from the competition between two nonlinear effects, Kerr self-focusing and plasma defocusing.
- **Kerr self-focusing:** As the ultrashort laser pulse propagates, the refractive index increases with intensity ($n = n_0 + n_2 I$), causing the beam to self-focus.
- **Plasma defocusing:** At high intensity, ionization produces free electrons; the plasma refractive index ($n_p = \sqrt{1 - n_e/n_c}$) decreases, leading to beam defocusing.
- **Result:** The balance between these two effects creates a stable filament, an ideal plasma channel for electron density diagnostics via Stark broadening.

Stark Broadening

Electronic density study

5. Electronic density diagnostic via Stark effect

Electronic density study

Stark broadening principles

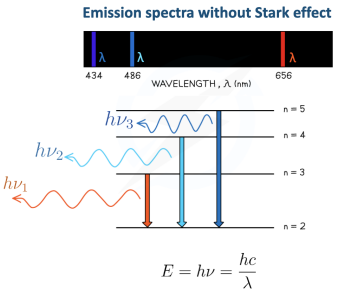

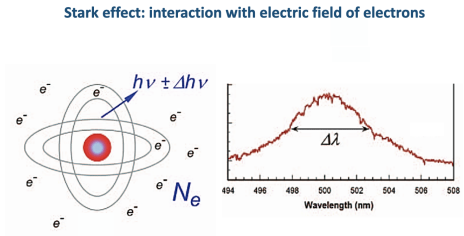

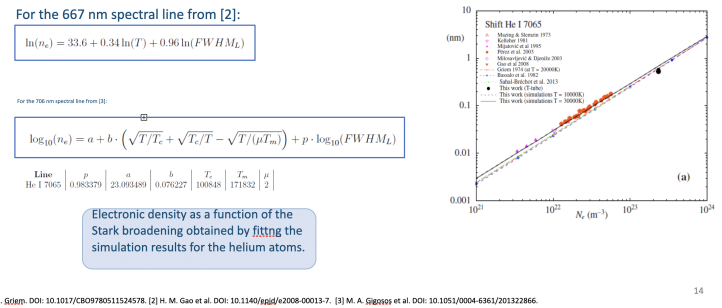

[1] H. R. Griem. DOI: 10.1017/CBO9780511524578. [2] H. M. Gao et al. DOI: 10.1140/epjd/e2008-00013-7. [3] M. A. Gigosos et al. DOI: 10.1051/0004-6361/201322866.

14

- Stark broadening happens when the light emitted by atoms in a plasma becomes wider (less sharp) because of the electric fields created by nearby charged particles, especially electrons.
- These electric fields disturb the atoms and slightly change the color (wavelength) of the light they emit.
- The stronger the electric field — meaning the higher the number of electrons — the wider the light line becomes.
- By measuring how wide the line is, scientists can find out how many electrons (or how dense) the plasma is.
- To translate the line broadening into an electron density value, we rely on empirical relationships derived for specific spectral lines.
- For the helium 667 nm line, the broadening is expressed as a function of temperature and full width at half maximum.

The camera pixel calibration and the raw spectral image of the plasma emission

6. Analysis and results

1º) Cameras spatial calibration

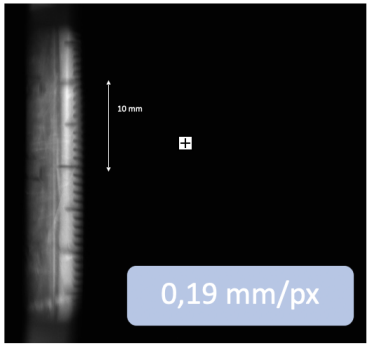

0th orden spectrometer camera (spatial calibration)

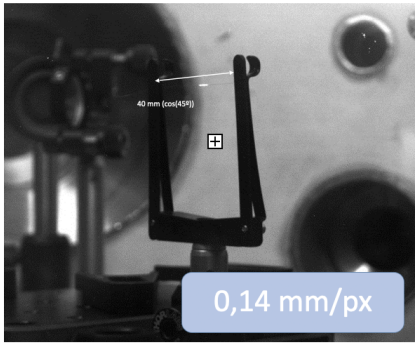

CMOS camera for filament image

2º) Camera spectral calibration

Rebuild of helium spectra

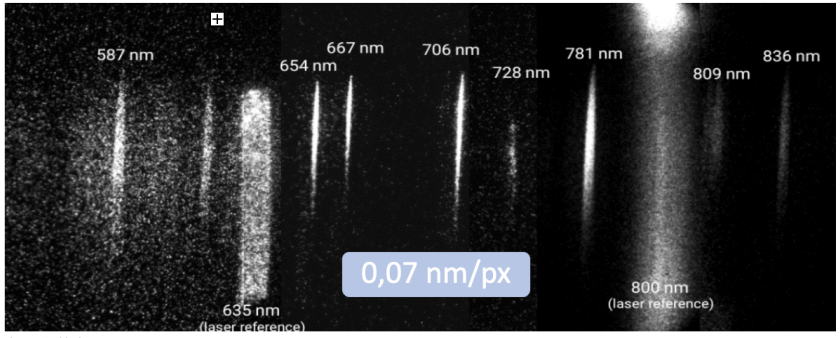

Theoretical helium spectra

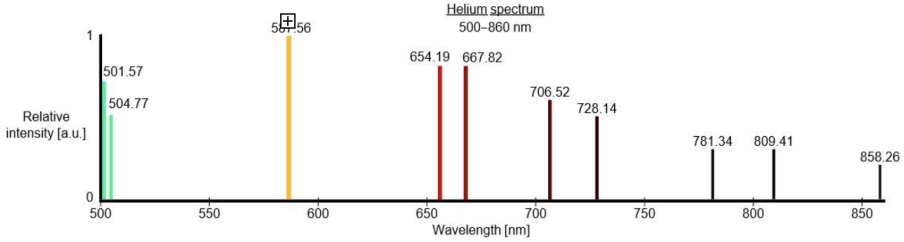

First, we calibrated the imaging and spectrometer systems to obtain the spatial and spectral resolutions of our setup.

The fitted Voigt function gives us both the line position and width, from which we determine the electron density.

6. Analysis and results

3º) Spectral image treatment

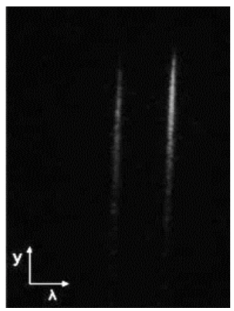

Signal treatments

Substract background and soften peaks

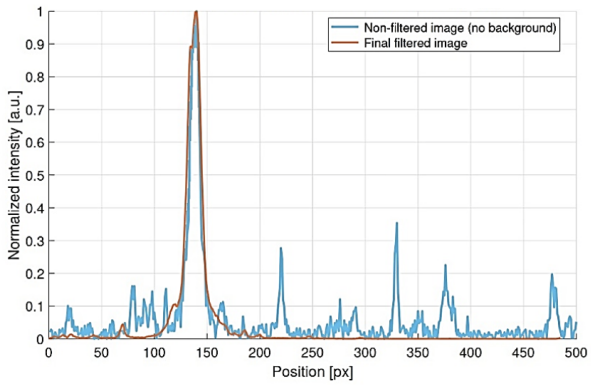

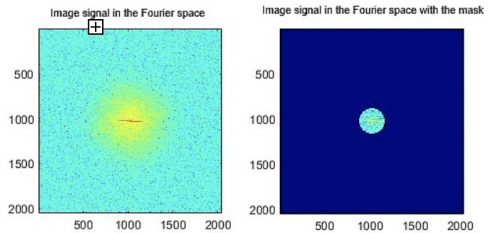

4º) Spectral line voigt fit

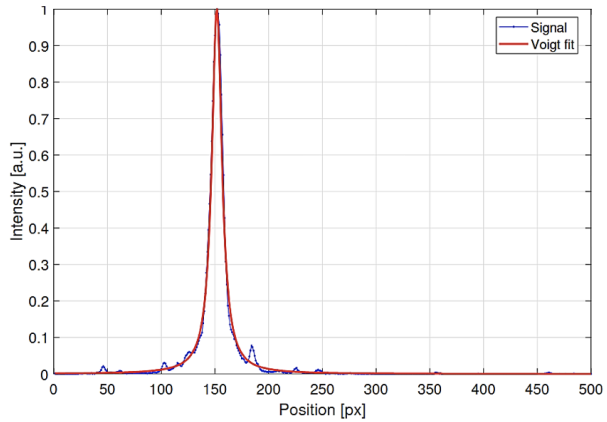

$$V(\lambda;\sigma,\gamma) \equiv \int_{-\infty}^{\infty} G(\lambda';\sigma)L(\lambda-\lambda';\Gamma)\,d\lambda'$$

After calibration, we process the spectral images to obtain intensity profiles.

Conclusions

- The **analytical framework** is based on an **operator formalism** that efficiently describes laser–plasma dynamics using mode amplitudes instead of full 3D fields.
- This approach provides a **unified and flexible description** of mode coupling, nonlinear feedback, and plasma oscillations, and can be extended to complex geometries or non-uniform plasmas.
- **Numerical (CFD) simulations:** Neutral gas density can be tuned by varying the inlet pressure, enabling precise control of plasma formation.
- The **Y-shaped capillary** geometry yields the most uniform and stable gas distribution for laser guiding.
- **Experimental diagnostics:** Electron density measured via Stark broadening of emission lines.
- Experimental observations confirm **controllable plasma density**.

Thank you for your attention!

Questions are welcome.

Note 1: Density perturbation is nonlinear

When an intense laser pulse propagates through a plasma, the rapidly oscillating field exerts a cycle-averaged **ponderomotive force** pushing electrons away from high-intensity regions. This produces a low-frequency density perturbation $\tilde{n}$, which modifies the refractive index and couples back to the laser field.

$$n(\mathbf{r},t) = n_0 + \tilde{n}(\mathbf{r},t), \quad \mathbf{v}(\mathbf{r},t) = \tilde{\mathbf{v}}(\mathbf{r},t),$$

$$\mathbf{E}(\mathbf{r},t) = \mathrm{Re}\{\Psi(\mathbf{r},z,t)e^{i(k_0 z-\omega_0 t)}\}, \quad U_p = \frac{e^2}{4m_e\omega_0^2}|\mathbf{E}|^2.$$

Continuity and momentum equations:

$$\partial_t n + \nabla\cdot(n\mathbf{v}) = 0,$$

$$m_e(\partial_t + \mathbf{v}\cdot\nabla)\mathbf{v} = -e\mathbf{E}_{\mathrm{low}} - m_e\nu\mathbf{v} - \nabla U_p - \frac{1}{n}\nabla P.$$

Linearizing and defining the displacement $\tilde{\mathbf{v}} = \partial_t\boldsymbol{\xi}$:

$$\tilde{n} = -n_0\nabla\cdot\boldsymbol{\xi},$$

$$m_e\partial_t^2\boldsymbol{\xi} + m_e\nu\partial_t\boldsymbol{\xi} = -e\mathbf{E}_{\mathrm{low}} - \nabla U_p - \frac{1}{n_0}\nabla P^{(1)}.$$

$$\nabla\cdot\mathbf{E}_{\mathrm{low}} = -\frac{e}{\varepsilon_0}\tilde{n} = \frac{en_0}{\varepsilon_0}\nabla\cdot\boldsymbol{\xi}.$$

Note 1: Density perturbation is nonlinear

Taking the divergence leads to the driven oscillator equation:

$$\partial_t^2 \tilde{n} + \nu \partial_t \tilde{n} + \omega_p^2 \tilde{n} = \frac{n_0}{m_e} \nabla^2 U_p + \frac{1}{m_e} \nabla^2 P^{(1)}, \quad \omega_p^2 = \frac{e^2 n_0}{\varepsilon_0 m_e}.$$

For a cold plasma ($P^{(1)} \approx 0$):

$$\partial_t^2 \tilde{n} + \nu \partial_t \tilde{n} + \omega_p^2 \tilde{n} = \frac{n_0}{m_e} \nabla^2 U_p.$$

In the quasi-static limit ($\omega \ll \omega_p$):

$$\tilde{n}(\mathbf{r}, t) \approx \frac{n_0(\mathbf{r})}{m_e \omega_p^2(\mathbf{r})} \nabla^2 U_p(\mathbf{r}, t) = \frac{\varepsilon_0}{4 m_e \omega_0^2} \nabla^2 |\mathbf{E}|^2.$$

This expression highlights that the density perturbation is nonlinear.
Including finite temperature:

$$(-\omega^2 + i\nu\omega + \omega_p^2 + \frac{\gamma k^2 k_B T_e}{m_e}) \tilde{n}(\mathbf{k}, \omega) = -\frac{n_0 k^2}{m_e} U_p(\mathbf{k}, \omega),$$

$$\tilde{n}(\mathbf{k}, \omega) = -\frac{n_0 k^2 / m_e}{\omega_p^2 - \omega^2 + i\nu\omega + 3k^2 v_{\mathrm{th}}^2} U_p(\mathbf{k}, \omega), \quad v_{\mathrm{th}} = \sqrt{\frac{k_B T_e}{m_e}}.$$

At relativistic intensities: $m_e \to \gamma m_e$ reduces $\tilde{n}$ response.
Projecting onto plasma eigenmodes $\{\phi_m\}$:

$$\tilde{n}_m(z, t) = \int \phi_m^*(\mathbf{r})\, \tilde{n}(\mathbf{r}, z, t)\, d^2 r \approx \int \phi_m^*(\mathbf{r})\, \nabla^2 \Big(\frac{e^2}{4 m_e \omega_0^2} |\Psi|^2 \Big)\, d^2 r.$$

The ponderomotive force thus acts as a nonlinear, intensity-dependent driver creating $\tilde{n} \propto \nabla^2 |E|^2$, coupling plasma and laser dynamics.

Note 2: The operator formalism is a mathematical tool

- The operator formalism is a **mathematical tool**, not a quantum assumption.
- It compactly describes mode evolution and coupling:

$$i\partial_z |\Psi\rangle = \hat{K} |\Psi\rangle , \qquad |\Psi\rangle = \sum_n A_n |\psi_n\rangle .$$

- $\hat{K}$ acts like a matrix coupling classical field modes ψ_n.
- For nonlinear plasma feedback:

$$i\partial_z |\Psi\rangle = (\hat{K} + \hat{N}[\Psi]) |\Psi\rangle ,$$

  where $\hat{N}[\Psi]$ is a **state-dependent operator**.
- This formalism keeps the physics clear: linear propagation $(\hat{K})$ + nonlinear response $(\hat{N}[\Psi])$.

Operators organize complex classical dynamics — they don't imply quantization.

The operator $\hat{\Omega}_p^2$ represents collective electron oscillations in plasma.

$$\partial_t \tilde{n} + \nabla \cdot (n_0 \tilde{\mathbf{v}}) = 0, \qquad m_e \partial_t \tilde{\mathbf{v}} = -e\mathbf{E}_{\text{low}}, \qquad \nabla \cdot \mathbf{E}_{\text{low}} = -\frac{e}{\varepsilon_0}\tilde{n}.$$

Eliminating $\tilde{\mathbf{v}}$ and $\mathbf{E}_{\text{low}}$ gives:

$$\partial_t^2 \tilde{n} + \mathcal{L}_{\text{plasma}} \tilde{n} = 0, \quad \mathcal{L}_{\text{plasma}} \phi_m = \omega_{p,m}^2 \phi_m.$$

Mode expansion:

$$\tilde{n}(\mathbf{r}, t) = \sum_m \delta n_m(t) \phi_m(\mathbf{r}), \quad \ddot{\delta n}_m + \omega_{p,m}^2 \delta n_m = 0.$$

Operator form:

$$\hat{\Omega}_p^2 = \sum_m \omega_{p,m}^2 \left|\phi_m\right\rangle \left\langle\phi_m\right|, \quad \hat{\Omega}_p^2 \left|\delta n\right\rangle = \sum_m \omega_{p,m}^2 \delta n_m \left|\phi_m\right\rangle.$$

Including damping and source terms:

$$\ddot{\delta n}_m + \nu_m \dot{\delta n}_m + \omega_{p,m}^2 \delta n_m = S_m(t),$$

with thermal and kinetic corrections:

$$\omega_{p,m}^2 \to \omega_{p,m}^2 + k_m^2 v_{\text{th}}^2, \quad \omega_{p,m} \to \omega_{p,m} - i\gamma_{L,m}.$$

$\hat{\Omega}_p^2$ generalizes the scalar plasma frequency to arbitrary geometries, linking microscopic plasma dynamics to macroscopic oscillations and enabling efficient operator-based modeling.

Note 5: Equivalence of Operator Formalism and Maxwell–Plasma PDEs

The operator-based formalism for LPWA is fully equivalent to the original Maxwell–plasma PDEs under a mode decomposition.
Maxwell–plasma PDEs:

$$\nabla^2 \mathbf{E} - \frac{1}{c^2}\frac{\partial^2 \mathbf{E}}{\partial t^2} = \mu_0 \frac{\partial^2 \mathbf{P}}{\partial t^2},$$
$$\frac{\partial^2 \delta n}{\partial t^2} + \omega_p^2 \delta n = -\frac{e n_0}{m_e} \nabla \cdot |\mathbf{E}|^2.$$

Mode expansions:

$$\mathbf{E}(\mathbf{r}_\perp, z, t) = \sum_n A_n(z)\psi_n(\mathbf{r}_\perp)e^{i(\beta_n z - \omega_0 t)}, \quad \delta n(\mathbf{r}_\perp, z, t) = \sum_m \delta n_m(z)\phi_m(\mathbf{r}_\perp)e^{-i\omega_0 t}.$$

Projected ODEs for mode amplitudes:

$$i\frac{dA_n}{dz} = \sum_m K_{nm}A_m - \frac{\omega_0^2}{2k_0 c^2}\sum_m N_{nm}[A]A_m,$$
$$\delta \ddot{n}_m + \omega_{p,m}^2 \delta n_m = -\sum_n \alpha_{mn}|A_n|^2,$$

with coupling coefficients

$$K_{nm} = \langle \psi_n | \hat{K} | \psi_m \rangle, \quad N_{nm}[A] = \langle \psi_n | \hat{N}[A] | \psi_m \rangle, \quad \alpha_{mn} = \langle \phi_m | \hat{\alpha} | \psi_n \rangle.$$

Operator form:

$$|\Psi\rangle = \sum_n A_n |\psi_n\rangle, \quad |\delta n\rangle = \sum_m \delta n_m |\phi_m\rangle,$$

$$i\partial_z |\Psi\rangle = \hat{K}|\Psi\rangle - \frac{\omega_0^2}{2k_0 c^2}\hat{N}[\Psi]|\Psi\rangle, \quad |\ddot{\delta n}\rangle + \hat{\Omega}_p^2 |\delta n\rangle = -\hat{\alpha}|\Psi|^2.$$

Expanding the operator equations reproduces the mode ODEs exactly, validating the operator formalism.

Note 6: Bloch-Floquet Theory and Operator Formalism in LPWA

LPWA produces periodic plasma structures along z with period $\Lambda \sim \lambda_p$, modulating density and refractive index:

$$n_0(\mathbf{r}_\perp, z) = n_{\mathrm{bkg}} + \delta n(z), \quad \delta n(z+\Lambda) = \delta n(z), \quad \epsilon(z+\Lambda) = \epsilon(z).$$

Fourier decomposition:

$$\delta n(z) = \sum_G \widetilde{n}_G e^{iGz}, \quad \Delta\epsilon(z) = \sum_G \widetilde{\Delta\epsilon}_G e^{iGz}, \quad G = 2\pi/\Lambda.$$

Bloch-Floquet solutions:

$$|\Psi(z)\rangle = e^{i\mu z} |u_\mu(z)\rangle, \quad |u_\mu(z+\Lambda)\rangle = |u_\mu(z)\rangle.$$

Single-harmonic modulation:

$$\Delta n(z) = \Delta n_0 \cos(G_0 z), \quad \frac{dA_+}{dz} = i\delta A_+ + i\kappa A_-, \quad \frac{dA_-}{dz} = -i\delta A_- + i\kappa^* A_+, \quad \mu^2 = \delta^2 + |\kappa|^2.$$

Operator formalism:

$$i\frac{\partial}{\partial z}|\Psi\rangle = \hat{K}(z)|\Psi\rangle - \frac{\omega_0^2}{2k_0c^2}\hat{N}[\Psi]|\Psi\rangle, \quad |\ddot{\delta n}\rangle + \hat{\Omega}_p^2(z)|\delta n\rangle = -\hat{\alpha}|\Psi|^2, \quad \hat{K}(z+\Lambda) = \hat{K}(z),$$

Periodic modulation couples modes separated by G, opening band gaps; nonlinear feedback can be included self-consistently.

Note 7: Full-Vector Operator Formalism for LPWA

- **Field expansion:** Electromagnetic field represented in vector mode basis: $\mathbf{E}(\mathbf{r}, z) = \sum_n A_n(z)\, \psi_n(\mathbf{r}) e^{i\beta_n z}$, including both transverse and longitudinal components.
- **Mode evolution:** Coupled operator equations:

$$i\partial_z \begin{pmatrix} |\Psi_T\rangle \\ |\Psi_L\rangle \end{pmatrix} = \begin{pmatrix} \hat{K}_{TT} & \hat{K}_{TL} \\ \hat{K}_{LT} & \hat{K}_{LL} \end{pmatrix} \begin{pmatrix} |\Psi_T\rangle \\ |\Psi_L\rangle \end{pmatrix} - \frac{\omega_0^2}{2k_0 c^2} \begin{pmatrix} \hat{N}_T[\Psi] \\ \hat{N}_L[\Psi] \end{pmatrix}.$$

- **Plasma response:** Density perturbation coupled to transverse and longitudinal fields:

$$|\ddot{\delta n}\rangle + \hat{\Omega}_p^2 |\delta n\rangle = -\hat{\alpha}_T |\Psi_T|^2 - \hat{\alpha}_L |\Psi_L|^2 - \hat{\alpha}_{TL}(\Psi_T^* \Psi_L + \Psi_L^* \Psi_T).$$

- **Operator interpretation:** $\hat{K}_{TT}$: transverse diffraction, $\hat{K}_{LL}$: longitudinal evolution, $\hat{K}_{TL}, \hat{K}_{LT}$: transverse-longitudinal coupling, $\hat{N}_{T,L}$: nonlinear self-action, $\hat{\alpha}_{TL}$: drives wake formation.
- **Advantages:** Unified compact description, mode–mode interactions, efficient numerics, extendable to quantum regime (χ_e).

Note 7: Applications of Full-Vector Operator Formalism in LPWA and Beyond

Laser–Plasma Wakefield Acceleration (LPWA)

- Self-consistent modeling of longitudinal wakefields (E_z) for particle acceleration.
- Describes cross-coupling between transverse laser modes and longitudinal plasma modes.
- Includes nonlinear effects: ponderomotive, relativistic, and mode-mode interactions.
- Facilitates laser profile optimization for improved acceleration and beam quality.

Plasma Photonics and High-Intensity Lasers

- Vectorial analysis of waveguides, plasma lenses, and structured capillaries.
- Models strong-field QED effects and radiation reaction in multi-PW lasers.
- Enables Bloch-Floquet analysis in periodic plasma or dielectric structures.

General Wave–Matter Interactions

- Analogous to multiband or spinor systems in condensed matter.
- Applicable to photonics, structured media, and nonlinear wave coupling.

Key Advantage: Efficiently describes transverse–longitudinal coupling, nonlinearities, and vectorial dynamics in a compact, operator-based framework.

Note 9: Hybrid Physics–AI Framework for LPWA

Operator-based LPWA dynamics:

$$i\frac{\partial |\Psi\rangle}{\partial z} = \hat{K}\,|\Psi\rangle - \frac{\omega_0^2}{2k_0c^2}\,\hat{N}[\Psi]\,|\Psi\rangle\,, \tag{1}$$

$$|\ddot{\delta n}\rangle + \hat{\Omega}_p^2\,|\delta n\rangle = -\hat{\alpha}\,|\Psi\rangle^2 \tag{2}$$

- $\hat{K}$: linear propagation, diffraction, and waveguide imperfections.
- $\hat{N}[\Psi]$: nonlinear plasma feedback (ponderomotive, relativistic effects).
- $\hat{\alpha}$: laser-driven ponderomotive source for plasma.
- $\hat{\Omega}_p^2$: natural plasma oscillation spectrum.

Physical interpretation:

- Laser drives plasma via $\hat{\alpha}$, plasma feeds back via $\hat{N}[\Psi]$.
- Bidirectional energy exchange generates wakefields.
- Linear operators $\hat{K}$ and $\hat{\Omega}_p^2$ define mode structure and oscillation spectrum.

Challenge: Nonlinear and nonlocal operators $\hat{N}[\Psi]$ and $\hat{\alpha}$ are computationally expensive in 3D simulations.

Note 9: Hybrid Physics–AI Framework for LPWA

Neural operator approximation: Neural operator models offer a powerful alternative. A neural operator $\mathcal{G}_\theta$ is a trainable functional mapping

$$\mathcal{G}_\theta : \Psi(\mathbf{r}, z) \mapsto \hat{N}[\Psi](\mathbf{r}, z), \tag{3}$$

parametrized by learnable weights θ. Once trained, $\mathcal{G}_\theta$ approximates the nonlinear operator $\hat{N}$ with high fidelity, enabling ultra-fast evaluation during simulation or control. Similarly, a second neural operator $\mathcal{A}_\phi$ can learn the mapping

$$\mathcal{A}_\phi : |\Psi|^2(\mathbf{r}, z) \mapsto \hat{\alpha}|\Psi|^2, \tag{4}$$

effectively reproducing the plasma source term driving wake formation. These models can be trained using data from high-fidelity particle-in-cell (PIC) or fluid simulations, where the true operator actions are known for various laser and plasma configurations.

Hybrid LPWA evolution:

$$i\frac{\partial |\Psi\rangle}{\partial z} = \hat{K}\,|\Psi\rangle - \frac{\omega_0^2}{2k_0 c^2}\,\mathcal{G}_\theta[\Psi]\,|\Psi\rangle\,, \tag{5}$$

$$|\ddot{\delta n}\rangle + \hat{\Omega}_p^2\,|\delta n\rangle = -\mathcal{A}_\phi[|\Psi|^2] \tag{6}$$

Advantages:

- *Reduced-order modeling*: AI replaces costly nonlinear operator evaluations.
- *Physics-informed learning*: retains Hermitian structure and plasma oscillation spectrum.
- *Predictive control*: differentiable operators enable gradient-based optimization.
- *Digital twin capability*: real-time simulation and control of LPWA experiments.

Note 9: Validation of the Operator Formalism

The operator formalism for laser–plasma interaction can be extra validated in the future:

- Comparing the operator-based evolution with full 2D/3D Maxwell–plasma PDE simulations.
- In the linear regime, verifying that plasma wave frequencies, mode dispersion, and wakefield amplitudes are correctly reproduced.
- Checking the conservation laws: energy and momentum are conserved in the linear limit due to Hermitian operators.

All of these validations will be performed in future work to confirm the accuracy and robustness of the operator approach.

Conclusion

- Laser–plasma dynamics desribed efficiently using **mode amplitudes** instead of full 3D fields.
- A **flexible, basis-independent framework** applies to complex geometries and non-uniform plasmas.
- Provides clear understanding of **mode coupling, nonlinear feedback, and plasma oscillations.**
- **Matrix techniques** applied for evolution, stability, and energy transfer analysis.
- **Self-consistent nonlinear effects** such as ponderomotive forces and self-modulation included.
- **Bloch-Floquet analysis** enabled for periodic plasma structures and mode bands.
- Framework prepared for **AI-assisted optimization** and physics-informed modeling.